Searches for Higgs boson pair production with the full LHC Run 2 dataset in ATLAS

Iván Sayago Galván on behalf of ATLAS collaboration

18/10/2021

Summary Slides

HH production at the LHC

Non-resonant: search for SM HH production targeting two mechanism:

- ggF sensitive to k_t and k_λ
- VBF sensitive to k_λ, k_V and k_{2V}

Resonant: search for BSM $X \rightarrow HH$ (ggF+VBF channel), where $m_X \in [251{,}3000]$ GeV

Gluon-gluon fusion (ggF) HH production $\sigma_{SM}^{ggF} = 31.05^{+2.2\%}_{-0.5\%}$ fb at $\sqrt{s} = 13$ TeV

Vector boson fusion (VBF) HH production $\sigma_{SM}^{VBF} = 1.723^{+0.03\%}_{-0.04\%} \pm 2.1\%$ fb at $\sqrt{s} = 13$ TeV

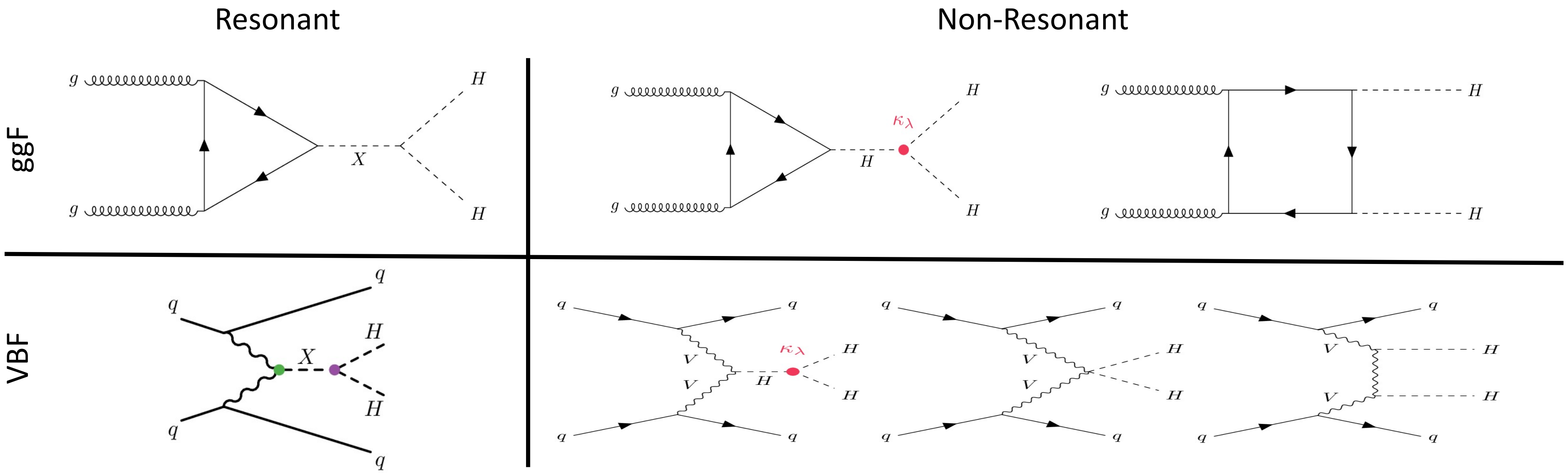

	bb	WW	ττ	ZZ	γγ
bb	33%				
WW	25%	4.6%			
ττ	7.4%	2.5%	0.39%		
ZZ	3.1%	1.2%	0.34%	0.076%	
γγ	0.26%	0.10%	0.029%	0.013%	0.0005%

HH decay modes and their total relative branching ratios 10.23731 / CYRM-2017-002

Non resonant HH production searches

Multivariate techniques used to separate signal from background resulting in improvements w.r.t increased luminosity along with better object reconstruction

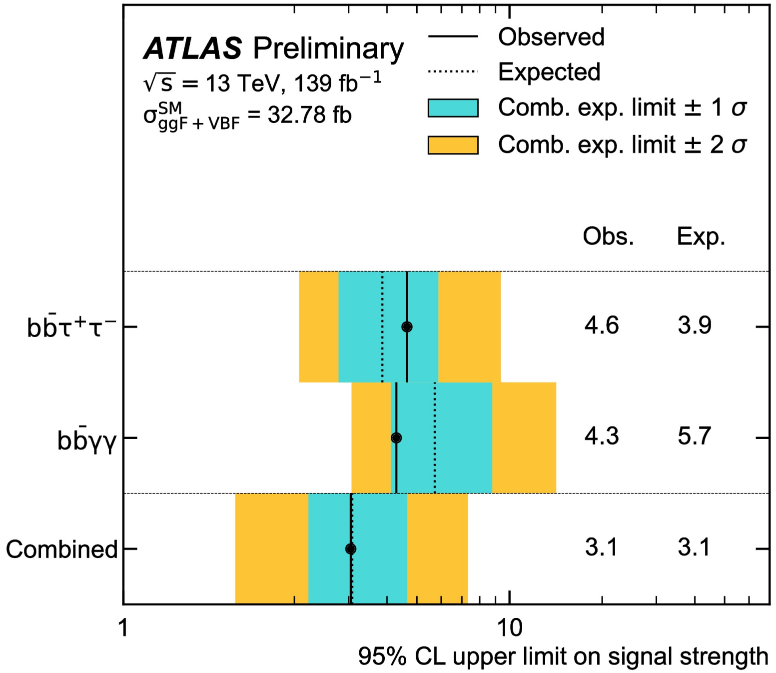

95% CL on k_λ(ggF+VBF)

Lumi	Observed	Expected
139 fb^{-1}	[-1.0,6.6]	[-1.2,7.2]

- ggF only considered for $b\bar{b}\ell\nu\ell\nu$
- $ggF + VBF$ are considered where, $b\bar{b}\gamma\gamma$ and $b\bar{b}\tau^+\tau^-$ being ggF optimized while $b\bar{b}b\bar{b}$ is VBF optimized
- Constraints are set on $k_\lambda = \lambda_{HHH}/\lambda_{HHH}^{SM}$ by $b\bar{b}\gamma\gamma$
- Constraints are set on σ_{ggF} by $b\bar{b}\ell\nu\ell\nu$, $b\bar{b}\tau^+\tau^-$ and $b\bar{b}\gamma\gamma$
- Additional constraints on $k_{2V} = c_{2v}/c_{2v}^{SM}$ by $b\bar{b}b\bar{b}$

*$b\bar{b}\ell\nu\ell\nu$ PLB 801(2020)135145 @ 139 fb^{-1}
*$b\bar{b}b\bar{b}$ JHEP07(2020)108 @ 126 fb^{-1}
*$b\bar{b}\tau^+\tau^-$ ATLAS-CONF-2021-030 @ 139 fb^{-1}
*$b\bar{b}\gamma\gamma$ ATLAS-CONF-2021-016 @ 139 fb^{-1}
*Combination ATLAS-CONF-2021-052 @ 139 fb^{-1}

Resonant HH production searches

The main hypotheses considered in ATLAS publications are:

- Narrow-width spin = 0 resonances
- Kluza-Klein graviton in the bulk Randall-Sundrul model with spin = 2 (only considered by $b\bar{b}b\bar{b}$)

Similar procedures w.r.t to the non-resonant searches

Each analysis lead the sensitivity in different m_X regions

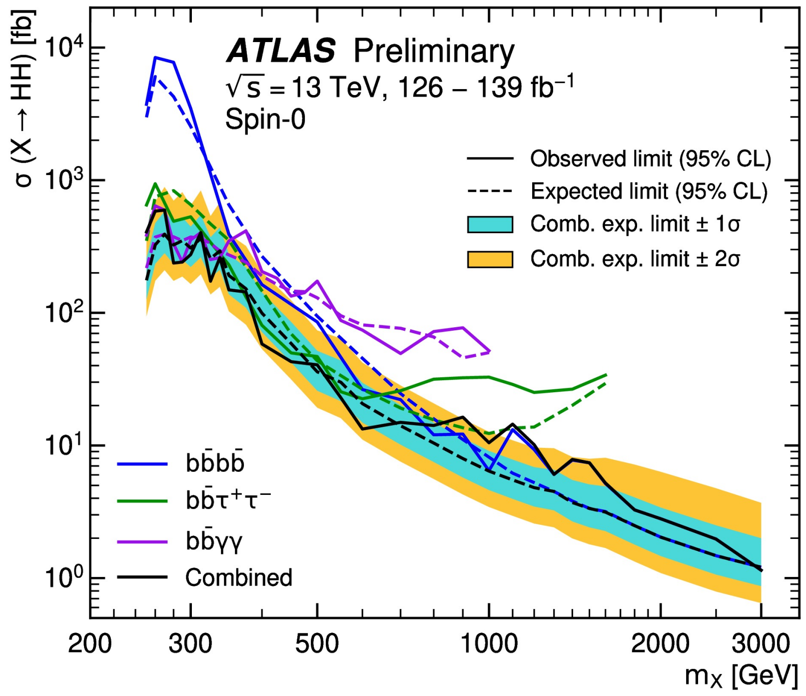

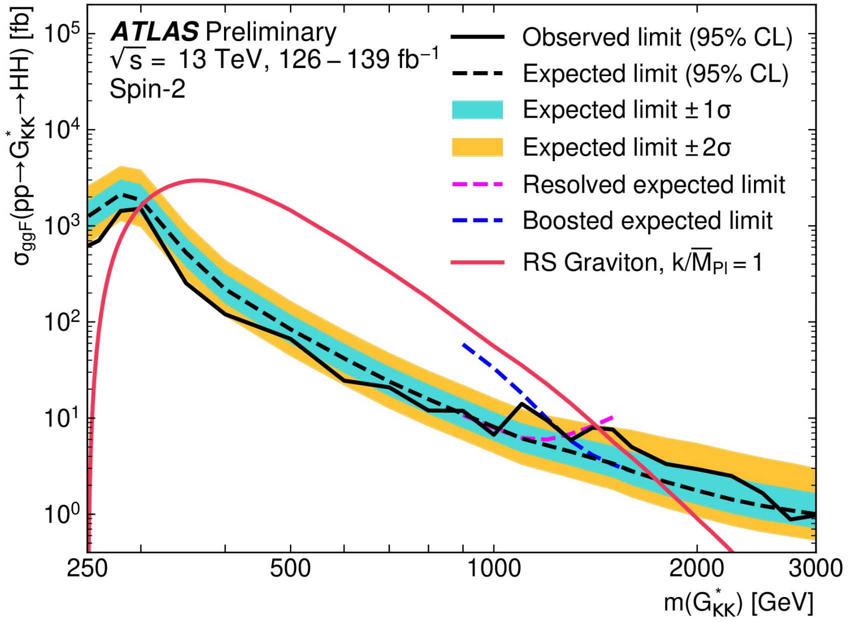

*$b\bar{b}b\bar{b}$ ATLAS-CONF-2021-035 @ 126 fb^{-1}

*$b\bar{b}\tau^+\tau^-$ ATLAS-CONF-2021-030 @ 139 fb^{-1}

*$b\bar{b}\gamma\gamma$ ATLAS-CONF-2021-016 @ 139 fb^{-1}

*Combination ATLAS-CONF-2021-052 @ 139 fb^{-1}

Detailed Slides

SM HH production at the LHC

Non-resonant HH production is predicted by the SM with a small predicted cross-section due to destructive interference. The observation of the HH production is a direct probe of the Higgs boson self-coupling along with the VVHH coupling.

Gluon-gluon fusion (ggF) HH production $\sigma_{SM}^{ggF} = 31.05^{+2.2\%}_{-0.5\%}$ fb at $\sqrt{s} = 13$ TeV

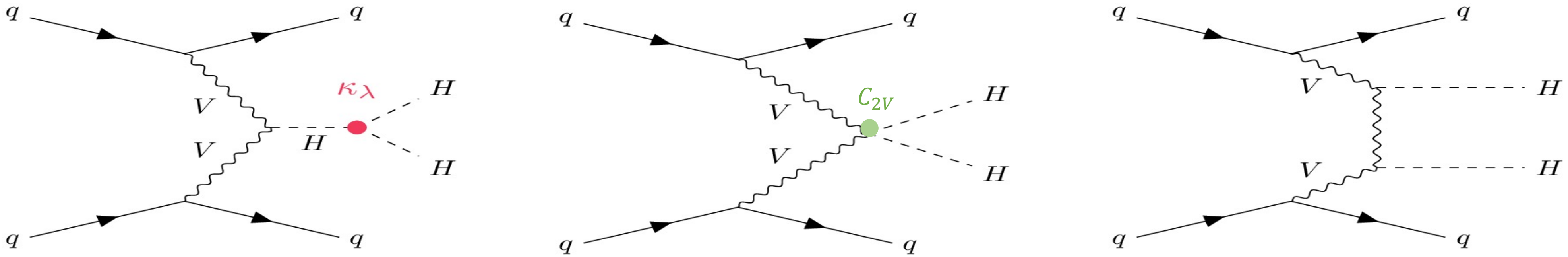

Vector boson fusion (VBF) HH production $\sigma_{SM}^{VBF} = 1.723^{+0.03\%}_{-0.04\%} \pm 2.1\%$ fb at $\sqrt{s} = 13$ TeV

Resonant HH production at the LHC

Resonant HH production through ggF is the main mode considered at the LHC. Public results using full Run 2 dataset are $b\bar{b}b\bar{b}$, $b\bar{b}\tau^+\tau^-$ and $b\bar{b}\gamma\gamma$. The main hypotheses considered in ATLAS publications are:

- Narrow-width spin = 0 resonances
- Kluza-Klein graviton in the bulk Randall-Sundrul model with spin = 2

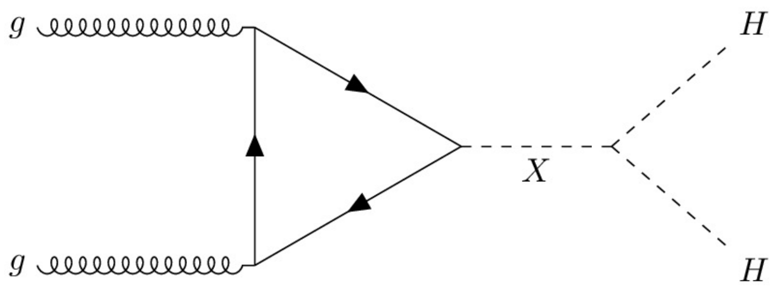

Resonant ggF HH production

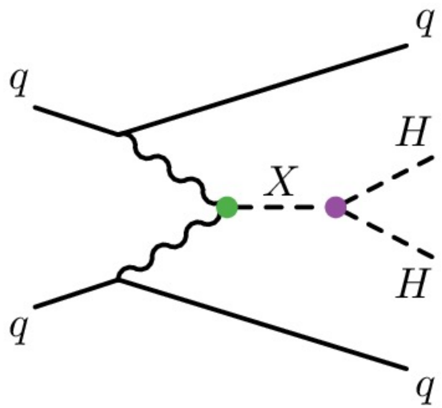

Resonant VBF HH production considered by $b\bar{b}b\bar{b}$ in JHEP07(2020)108

Non-Resonant production

Decay channel and Run 2 data set public results

HH decay modes and their total relative branching ratios
10.23731 / CYRM-2017-002

	bb	WW	ττ	ZZ	γγ
bb	33%				
WW	25%	4.6%			
ττ	7.4%	2.5%	0.39%		
ZZ	3.1%	1.2%	0.34%	0.076%	
γγ	0.26%	0.10%	0.029%	0.013%	0.0005%

- ggF only considered for $b\bar{b}\ell\nu\ell\nu$
- $ggF + VBF$ are considered where, $b\bar{b}\gamma\gamma$ and $b\bar{b}\tau^+\tau^-$ being ggF optimized while $b\bar{b}b\bar{b}$ is VBF optimized
- Constraints are set on $k_\lambda = \lambda_{HHH}/\lambda_{HHH}^{SM}$ by $b\bar{b}\gamma\gamma$ and $b\bar{b}\tau^+\tau^-$
- Constraints are set on σ_{ggF} by $b\bar{b}\ell\nu\ell\nu$, $b\bar{b}\tau^+\tau^-$ and $b\bar{b}\gamma\gamma$
- Additional constraints on $k_{2V} = c_{2v}/c_{2v}^{SM}$ by $b\bar{b}b\bar{b}$

*$b\bar{b}\ell\nu\ell\nu$ PLB 801(2020)135145 @ 139 fb^{-1}
*$b\bar{b}b\bar{b}$ JHEP07(2020)108 @ 126 fb^{-1}
*$b\bar{b}\tau^+\tau^-$ ATLAS-CONF-2021-030 @ 139 fb^{-1}
*$b\bar{b}\gamma\gamma$ ATLAS-CONF-2021-016 @ 139 fb^{-1}
*Combination ATLAS-CONF-2021-052 @ 139 fb^{-1}

VBF $HH \rightarrow b\bar{b}b\bar{b}$ (126 fb^{-1})

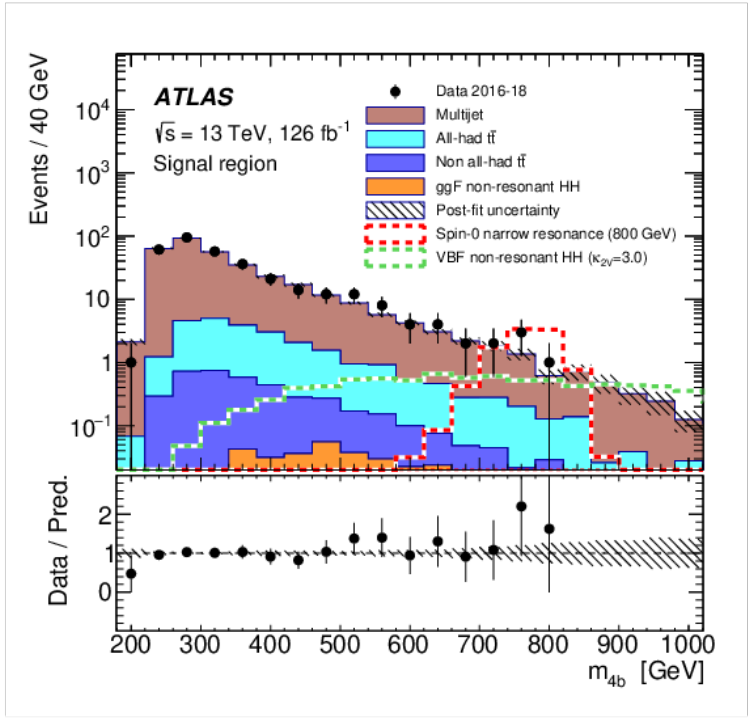

- The analysis is optimized for searches in the VBF HH production mode
- ggF HH production is normalized to the SM expectation and added to the background
- Multijet data-driven background makes up for the 95% of the total background

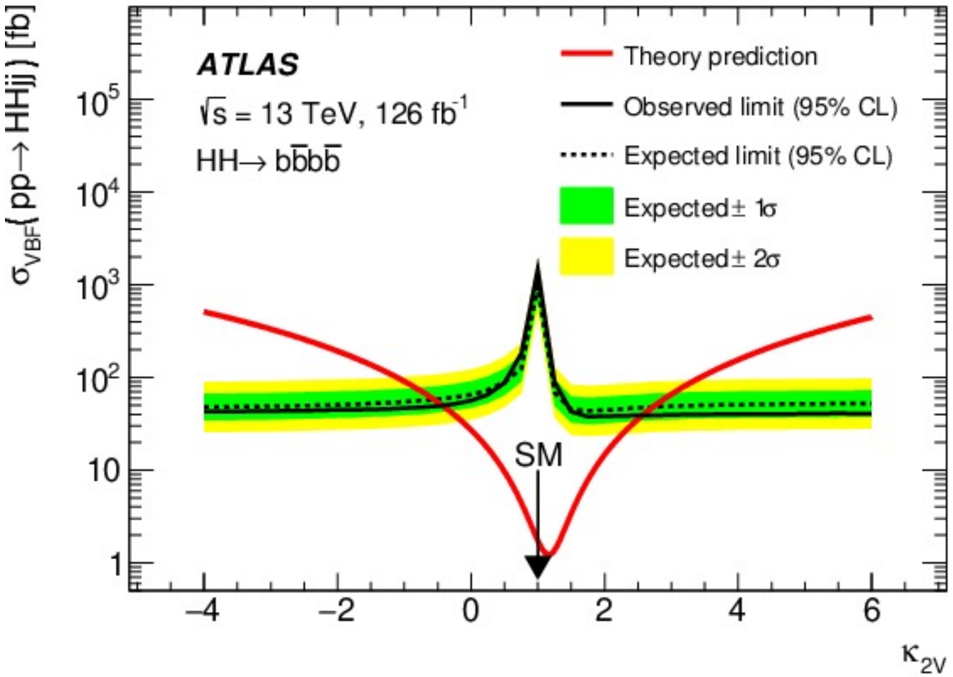

95% CL limit on $\sigma_{VBF}/\sigma_{VBF}^{SM}$

Expected	Observed
550	840

95% CL allowed interval on k_{2V}

Expected	Observed
[-0.55,2.72]	[-0.43,2.56]

JHEP07(2020)108

$HH \to b\bar{b}\ell\nu\ell\nu (139\ \mathrm{fb}^{-1})$

- One $H \to b\bar{b}$ and other $H \to WW^*, ZZ^*, \tau\tau$
- Events requiring at least 2 b-jets and exactly 2 leptons
- Signal background separation performed with a multi-class neural network trained with $HH \to b\bar{b}WW^*$
- Events divided in 4 categories:
  - HH
  - Top
  - $Z - \ell\ell$
  - $Z - \tau\tau$
- Discriminant d_{HH} is built from these categories

95% CL on $\sigma_{HH}/\sigma_{HH}^{SM}$ (ggF)

Channel	Observed	-1σ	Expected	$+1\sigma$
$b\bar{b}\ell\nu\ell\nu$	40	20	29	43

LB 801(2020)135145

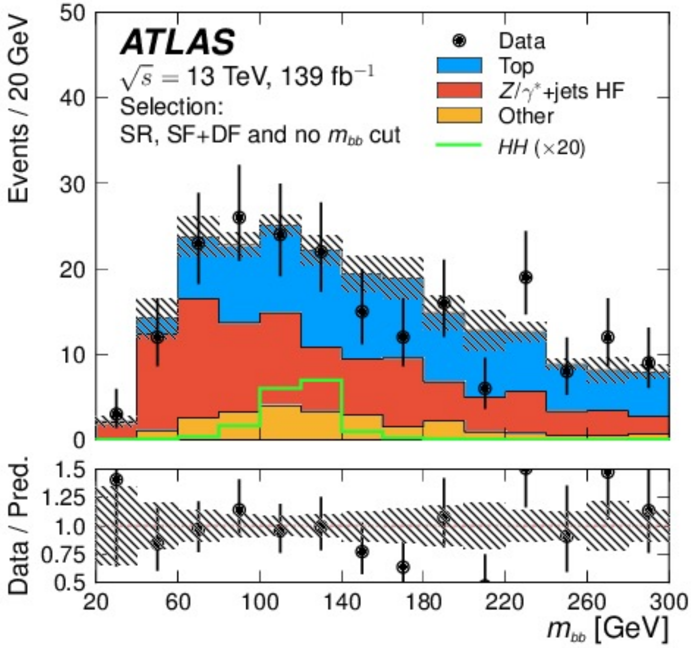

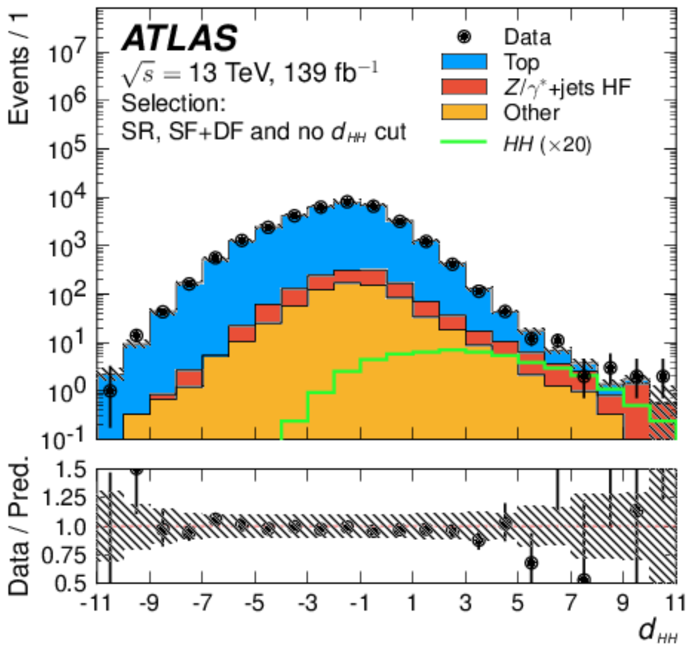

$HH \rightarrow b\bar{b}\tau^{+}\tau^{-}$ (139 fb^{-1})

- Possible final states: $\tau_{had}\tau_{had}$ and $\tau_{lep}\tau_{had}$ (lepton can be electron or muon)
- Three signal regions (SRs) based on di-τ decay and trigger categories (two τ_{had} and $e/\mu + \tau_{had}$)
- Main background are fakes τ_{had} from misidentified jets (multijet, W+jets and $t\bar{t}$) that are estimated using data-driven techniques
- Contributions from non-fake backgrounds are evaluated using MC samples
- Signal / background separation is based on multivariate (MVA) techniques:
  - Neural Network (NN) and Boosted Decision Trees (BDTs)
  - Input variables depending on the channel

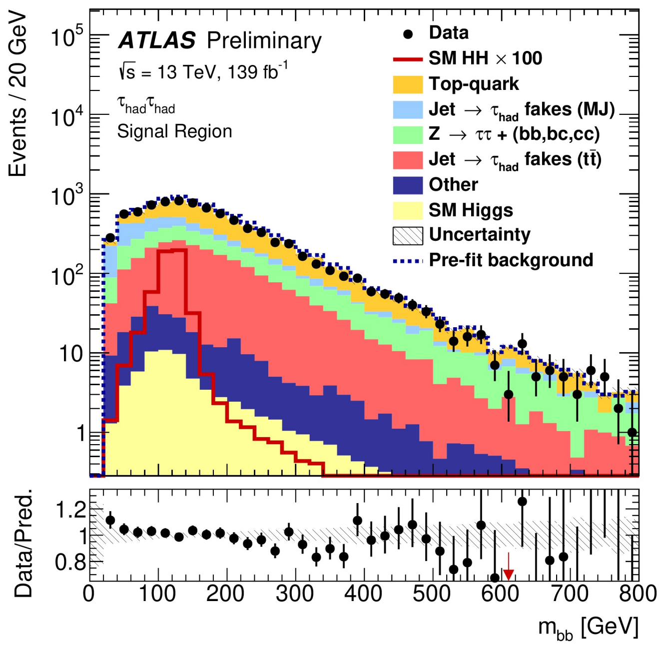

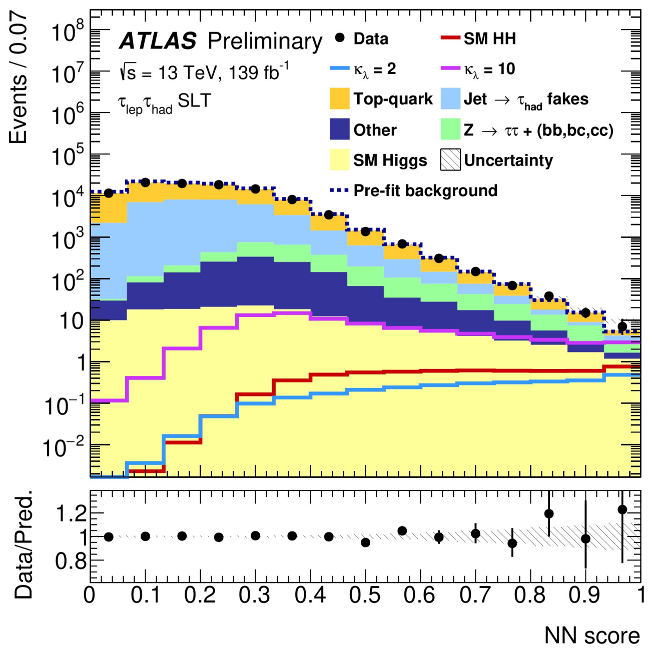

ATLAS-CONF-2021-030

$HH \rightarrow b\bar{b}\tau^{+}\tau^{-}$ (139 fb^{-1})

- MVA score is used as final discriminant in the fit

95% CL on $\sigma_{HH}/\sigma_{HH}^{SM}$ (ggF+VBF)

Channel	Observed	-1σ	Expected	$+1\sigma$
$\tau_{\text{had}}\tau_{\text{had}}$	4.95	3.19	4.43	6.17
$\tau_{\text{lep}}\tau_{\text{had}}$	9.16	5.66	7.,86	10.9
Combined	4.65	2.79	3.87	5.39

95% CL on k_{λ}(ggF+VBF)

Lumi	Observed	Expected
139 fb^{-1}	[-2.4,9.2]	[-2.0,9.0]

- Factor ~4 improvement compared to 36 fb^{-1} (PRL 121(2018)191801):
    - Previous result exp. 14.8, obs. 12.7
    - Half due to luminosity increase
    - Half due to improved τ_{had} and b-jet reconstruction and identification and analysis-level improvements

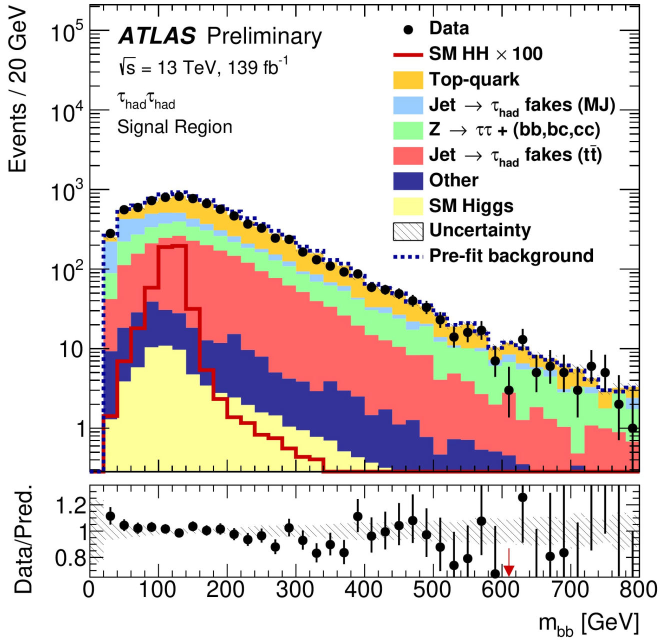

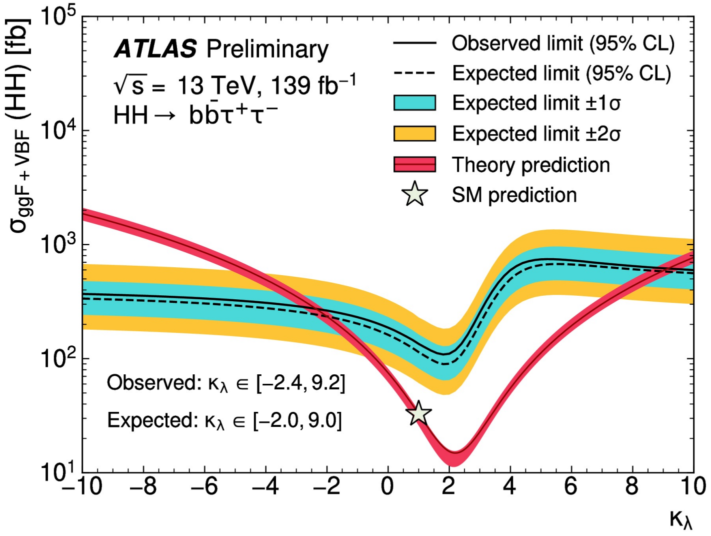

ATLAS-CONF-2021-030 ATLAS-CONF-2021-052

$HH \rightarrow b\bar{b}\gamma\gamma (139\ \text{fb}^{-1})$

- Event pre-selection is based on di-photon trigger, 2 good photons and b-jet requirements
- Events are divided into low di-Higgs mass region and high di-Higgs mass region:
  - Low mass region aims large $|k_\lambda|$ searches
  - High mass region is more sensitive to SM and small values of $|k_\lambda|$
- BDTs are trained on $k_\lambda = 1{,}10$ against main backgrounds ($\gamma\gamma$+jets, $t\bar{t}H$, ZH and WH)
- A total of four categories are defined based on:
  - Low mass region:
    - Tight BDT score cut
    - Loose BDT score cut
  - High mass region:
    - Tight BDT score cut
    - Loose BDT score cut

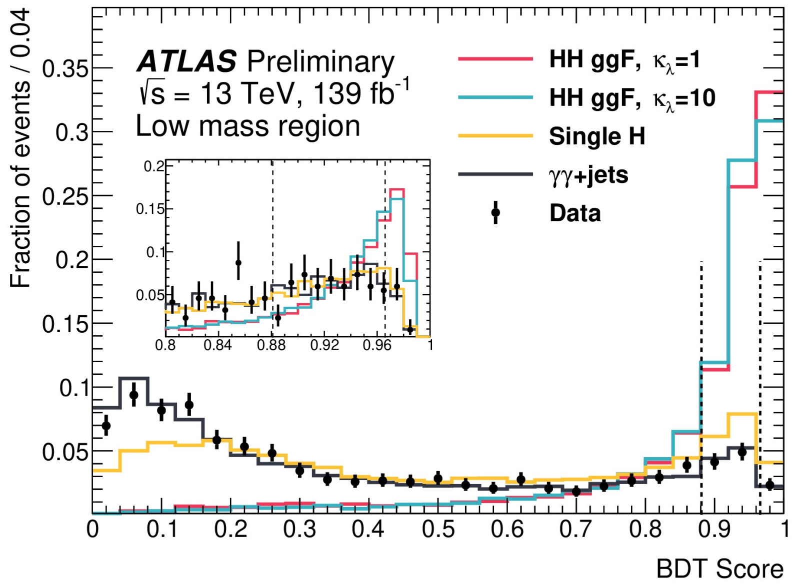

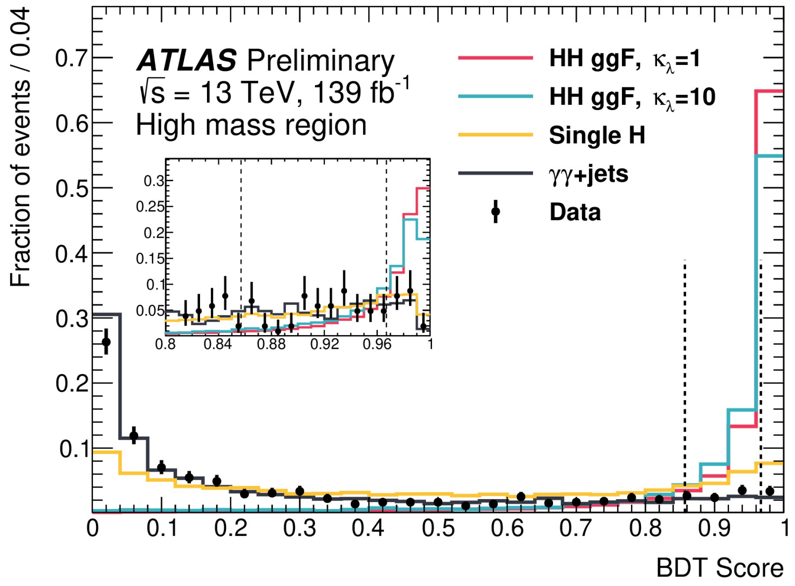

ATLAS-CONF-2021-016 ATLAS-CONF-2021-052

$HH \rightarrow b\bar{b}\gamma\gamma$ (139 fb^{-1})

- Signal extracted from fitting the $m_{\gamma\gamma}$ distribution
- Signal and single-Higgs background $m_{\gamma\gamma}$ are modelled using a double-sided Crystal Ball function
- Continuum $\gamma\gamma$ background is modelled using an exponential function fitting the data sidebands

95% CL on $\sigma_{HH}/\sigma_{HH}^{SM}$ (ggF+VBF)

Channel	Observed	Expected
$b\bar{b}\gamma\gamma$	5.5	4.1

95% CL on k_λ(ggF+VBF)

Lumi	Observed	Expected
139 fb^{-1}	[-2.4,7.7]	[-1.5,6.7]
36 fb^{-1}	[-5.8,12.0]	[-5.0,12.0]

- A factor 4 improvement w.r.t previous result JHEP(2018)040 due to improved luminosity, b-jet reconstruction and analysis optimizations

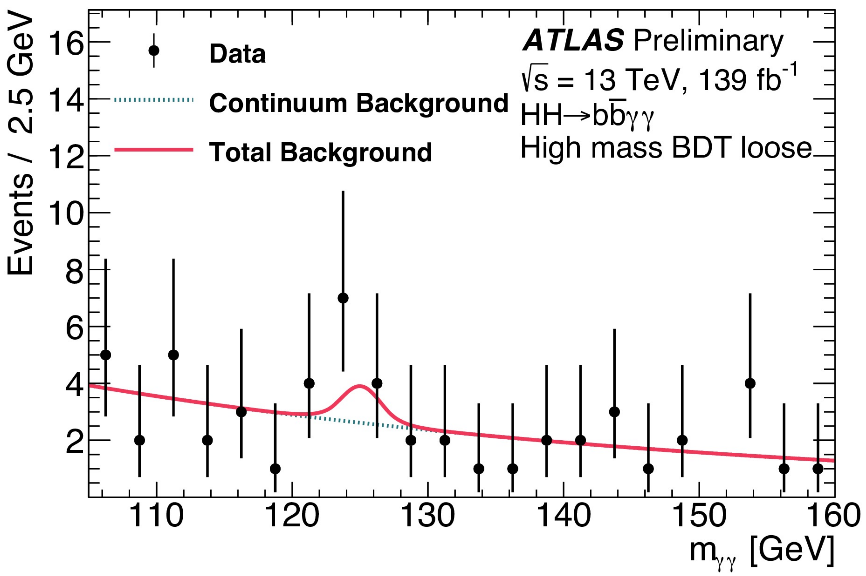

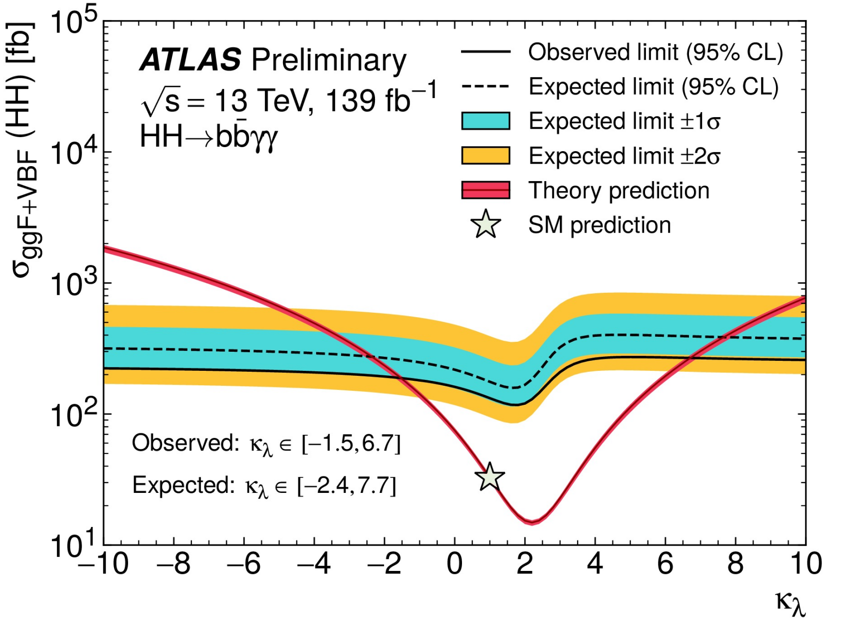

ATLAS-CONF-2021-016 ATLAS-CONF-2021-052

Combination Summary

- Two analyses already improving previous combination ($\sigma_{HH}/\sigma_{HH}^{SM}$ = 6.9 Obs, 10 Exp)
- More results with full Run 2 dataset yet to be published. Stay tuned!

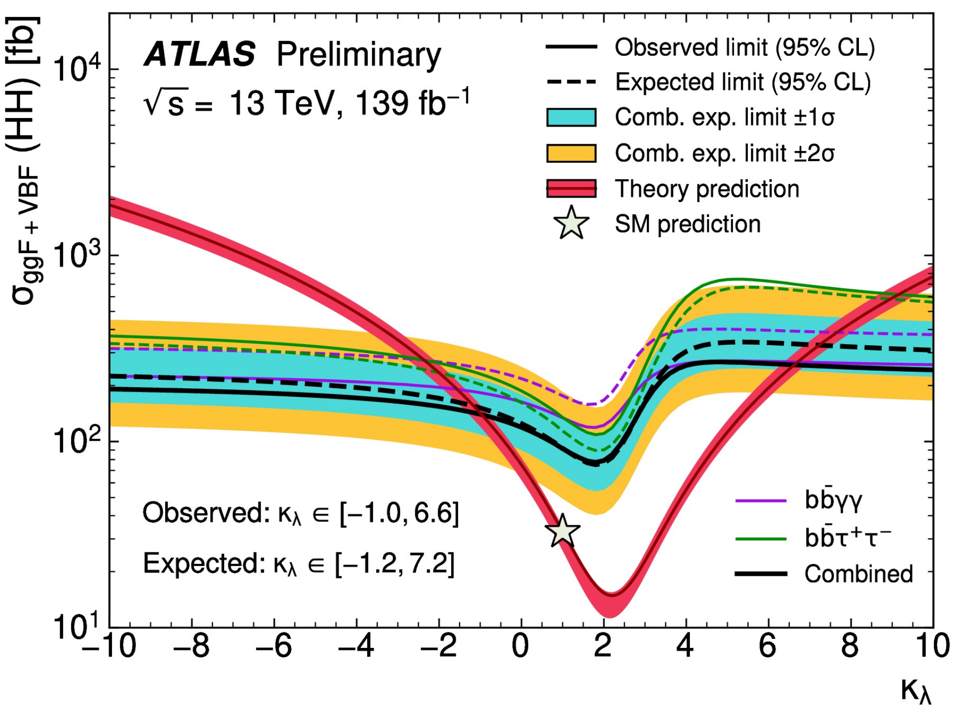

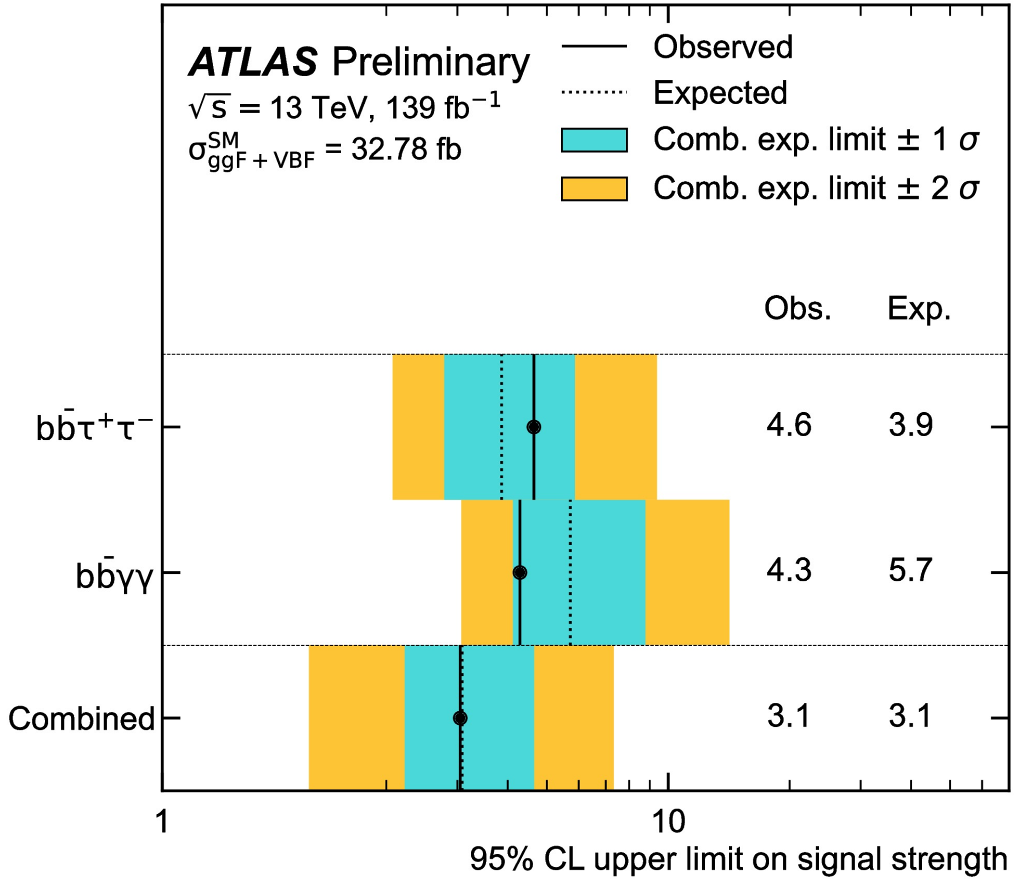

ATLAS-CONF-2021-052

Resonant production

Resonant $HH \to b\bar{b}b\bar{b}$ ($126\ \text{fb}^{-1} - 139\ \text{fb}^{-1}$)

Resolved:

- Resonances ranging $m_X \in [251,1500]$ GeV
- Four classes based on triggers: high-E_T b-jet, 2 b-jet+jet, high- E_T and 2b-jet+2jets
- BDTs are used to pair b-jets
- Data-driven background ($\sim 95\%$ multijet, rest $t\bar{t}$):
  - NN reweighting correction applied

Boosted:

- Resonances ranging $m_X \in [900,3000]$ GeV
- Atleast two large-radius jet requirement
- Three categories 2b, 3b and 4b where a large-radius jet is matched to 1 or 2 b-tagged track jets
- Multijet background is data-driven
- $t\bar{t}$ backround is simulated

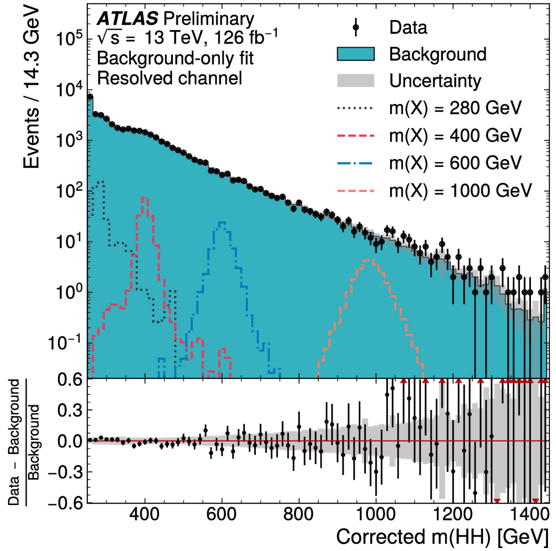

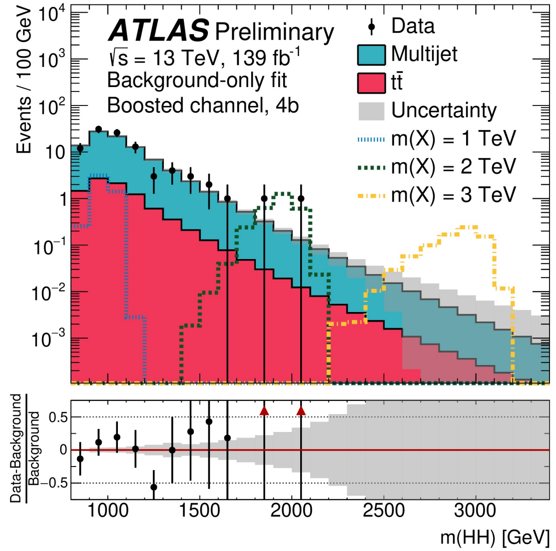

ATLAS-CONF-2021-035

Resonant $HH \rightarrow b\bar{b}b\bar{b}$ $(126\ \text{fb}^{-1} - 139\ \text{fb}^{-1})$

- Signal Regions are defined in the m_{H_1}, m_{H_2} plane
- Variable m_{HH} is used as discriminant variable

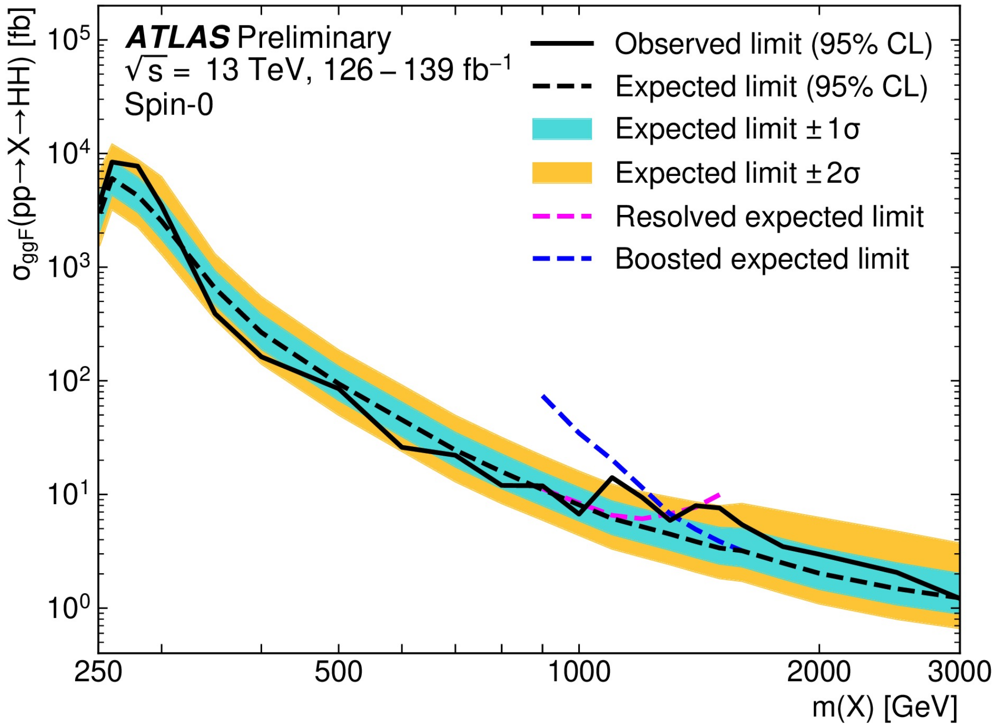

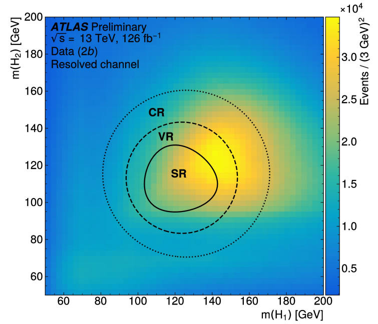

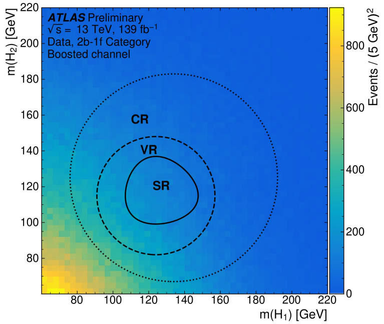

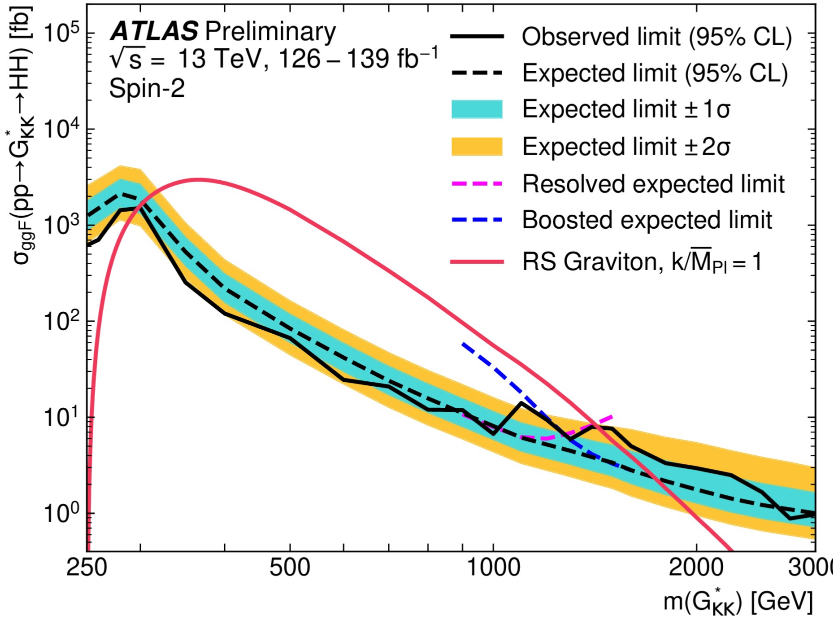

Bulk Randal—Sundrum model graviton excluded $(k/\bar{M}_{Pl} = 1)$ at 95% CL

	Mass Range (GeV)
ATLAS-CONF-2021-035	298-1440
PLB800(2020)135103	310-1380

ATLAS-CONF-2021-035

Resonant $HH \rightarrow b\bar{b}\tau^{+}\tau^{-}(139\ \mathrm{fb}^{-1})$

- Signal / background separation is based on a parametric neural network (PNNs)
  - Resonance mass is parametrized in the NN
  - Input variables depending on the channel
- MVA score is used as final discriminant in the fit
- Local excess at 1.0 (1.1) TeV in the $\tau_{\mathrm{had}}\tau_{\mathrm{had}}$ ($\tau_{\mathrm{lep}}\tau_{\mathrm{had}}$) channel of 2.8$\sigma$ (1.5σ)
- Combined excess at 1 TeV local (global) of 3.0σ (2.0σ)

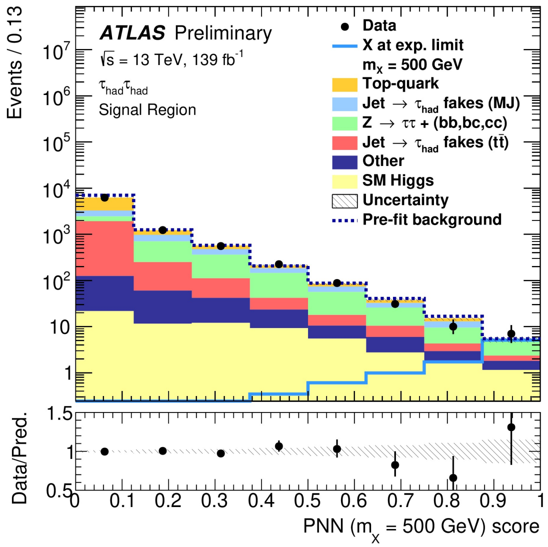

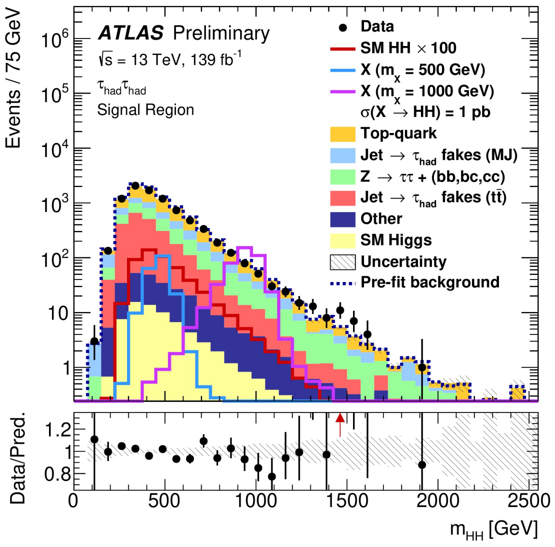

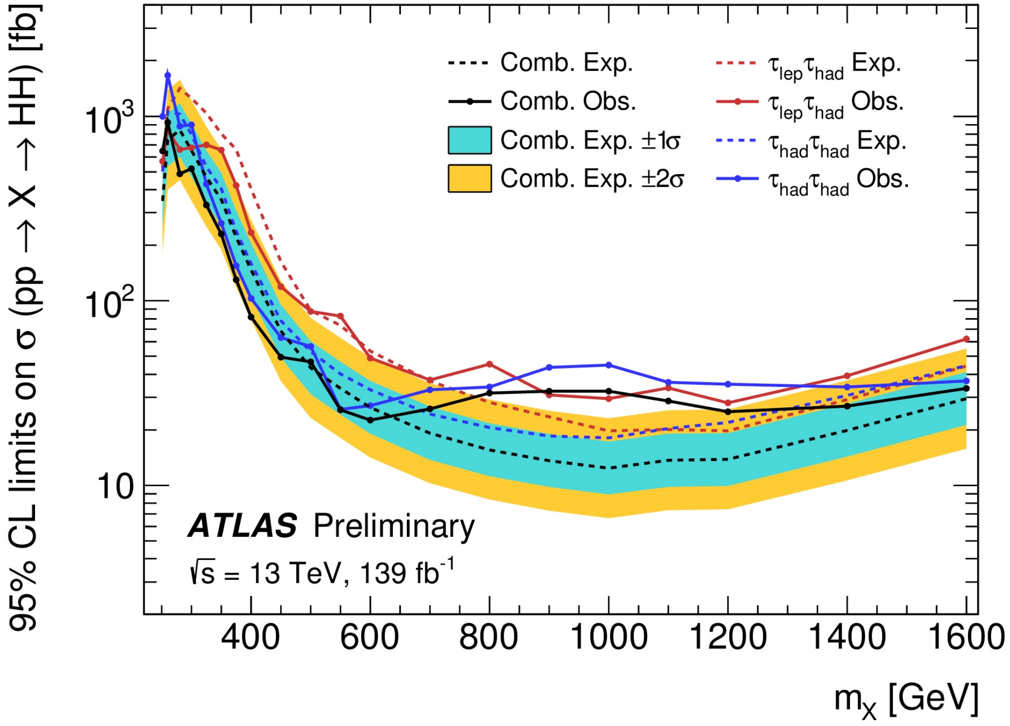

ATLAS-CONF-2021-030

Resonant $HH \rightarrow b\bar{b}\gamma\gamma$ (139 fb^{-1})

- BDTs trained separately against $\gamma\gamma$ and single-Higgs background and combined in quadrature:
  - All resonances are merged as signal for the BDT training and reweighted to match m_{HH} background distribution
- A category defined for each resonance based on:
  - BDT Score cut
  - Resonance mass
- $m_{\gamma\gamma}$ variable is used as discriminant

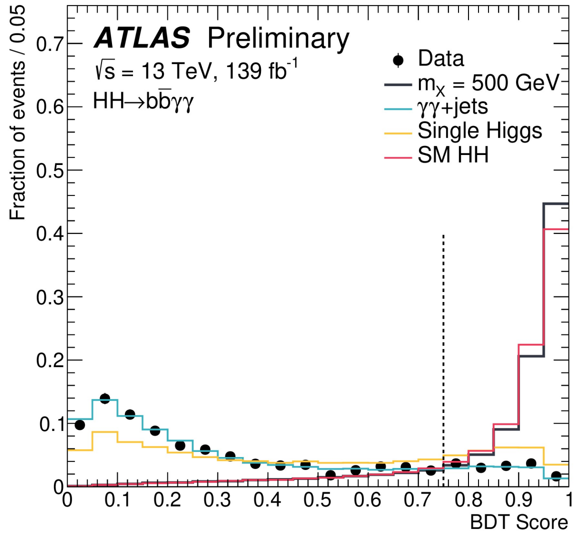

σ upper limit at 95% CL	Observed	Expected
ATLAS-CONF-2021-016	610-47	360-43
JHEP11(2018)040	1140-120	900-150

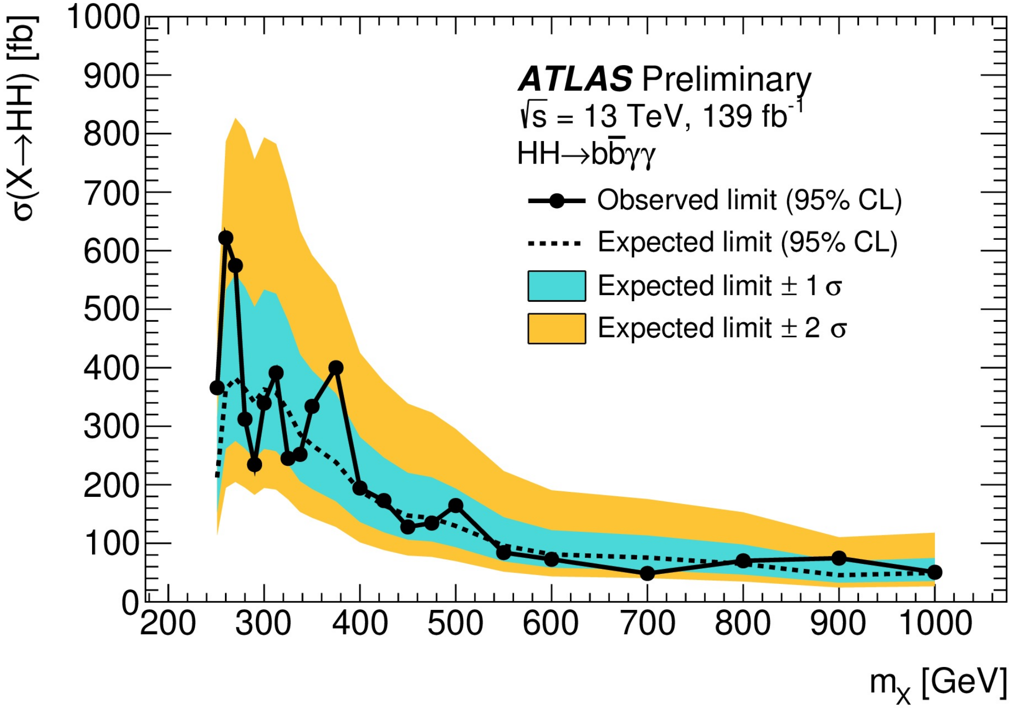

ATLAS-CONF-2021-016

Summary of resonant spin-0 limits

- The three shown analyses leads the sensitivity in different m_X regions
- All three analyses are already improving the previous combination

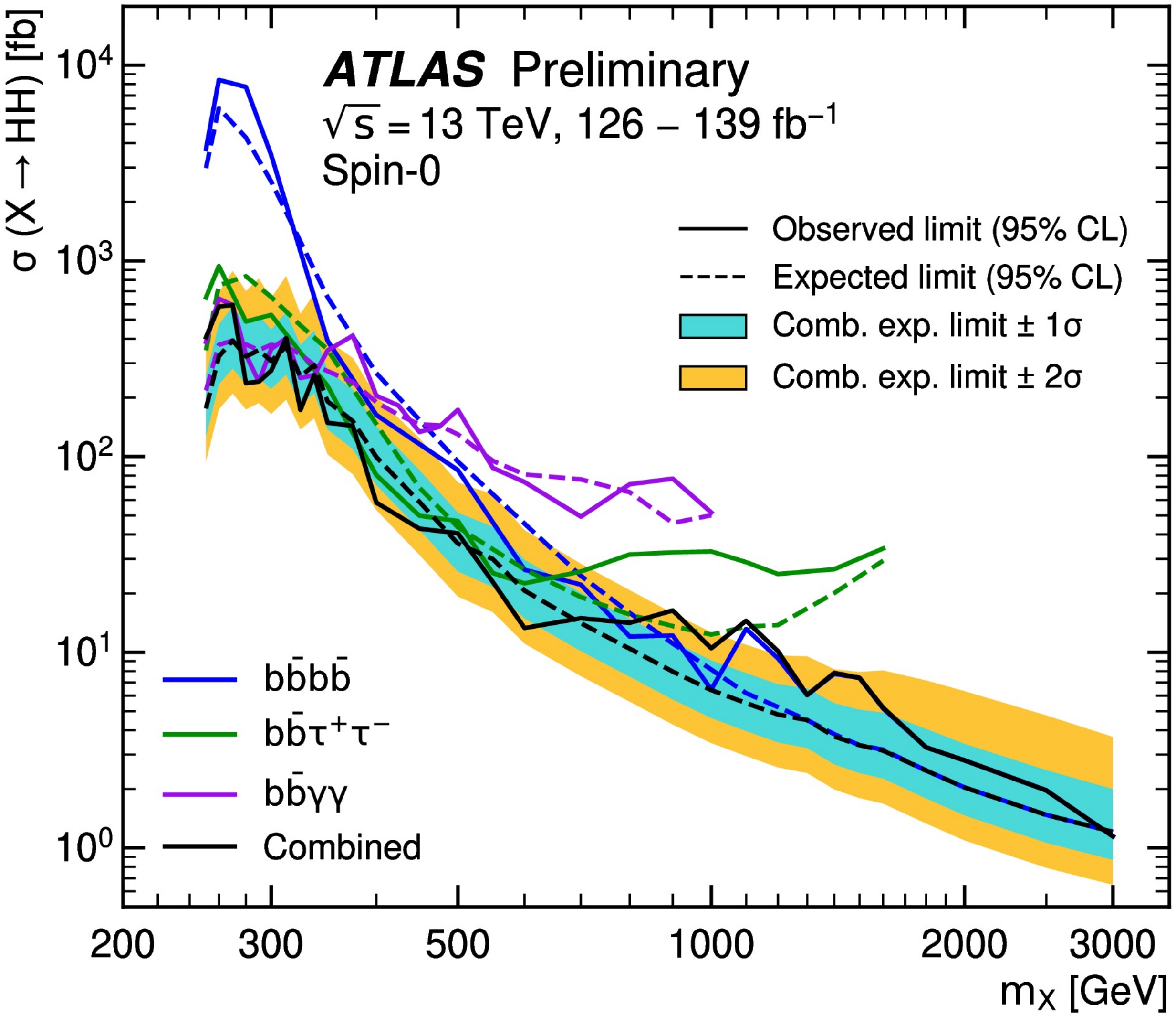

ATLAS-CONF-2021-052

Conclusions

- Three analyses have been updated to use full Run 2 dataset : $b\bar{b}b\bar{b}$, $b\bar{b}\tau^+\tau^-$ and $b\bar{b}\gamma\gamma$
- All three analyses represent improvements a part from the increased luminosity:
  - Better object reconstruction
  - Better techniques used in the analyses
- All new analyses are improving the previous 36fb^{-1} combination results
- Stay tune for more results and their combinations!

Back up